

# Specification and operation Expert consensus for optical coherence tomography angiography examination in small animals (2025)

Yi Shao<sup>1</sup>, Dan Ji<sup>2</sup>, Biao Yan<sup>1</sup>, *Expert Workgroup of Guidelines for Application of Artificial Intelligence in OCTA Image Analysis and Ocular Disease Diagnosis (2025); Ophthalmic Imaging and Intelligent Medicine Branch of Chinese Medicine Education Association; Ophthalmology Committee of International Association of Translational Medicine; Ophthalmology Committee of International Association of Intelligent Medicine; Chinese Ophthalmic Imaging Study Groups*

<sup>1</sup>Department of Ophthalmology, Shanghai General Hospital, Shanghai Jiao Tong University School of Medicine, National Clinical Research Center for Eye Diseases, Shanghai 200080, China;

<sup>2</sup>Department of Ophthalmology, Xiangya Hospital, Zhongnan University, Changsha, Hunan 410000, China;

**Corresponding authors:** Yi Shao, E-mail: freebee99@163.com; Dan Ji, E-mail: jidan222@163.com; Biao Yan, E-mail: yanbiao1982@126.com

**Key words:** Optical coherence tomography, vascular microcirculation, OCT, OCTA, retina, cornea

**Received:** November 25, 2024

**Accepted:** March 12, 2025

**Published:** June 21, 2025

**Copyright:** © 2025 Shao et al. This is an open access article distributed under the terms of the [Creative Commons Attribution License](https://creativecommons.org/licenses/by/3.0/) (CC BY 3.0), which permits unrestricted use, distribution, and reproduction in any medium, provided the original author and source are credited.

## ABSTRACT

Optical coherence tomography (OCT) and optical coherence tomography angiography (OCTA) have rapidly advanced over the past two decades as non-contact imaging techniques for tomographic analysis of intraocular tissue structures. Their applications in diagnosing and studying retinal diseases and glaucoma have revealed their unique clinical value. With the continuous innovation of technology, there are many

brands of clinical instruments based on OCT/OCTA, and the iterative update is fast, so we need to improve the application level. In the field of small animal research, challenges arise due to the anatomical differences and experimental requirements between small animals and humans. Moreover, anterior segment and retinal OCT/OCTA technologies represent high-resolution three-dimensional optical detection methods *in vivo*, posing difficulties for existing clinical instruments to meet the rigorous scientific and accuracy standards demanded by scientific research and efficacy evaluations. At the same time, the complexity of animal experiments, the diversity of scientific research tasks, and the constraints such as limited training time, insufficient experience in instrument operation, compared to clinical settings can lead to suboptimal OCT/OCTA outcomes for some research. To address this practical challenge, this guide summarizes the technical principles, operation procedures and experimental precautions related to OCT/OCTA for the anterior segment and retina in small animals. It also outlines the reference standards for corneal, retinal, and microvascular indicators across different animal models using OCT/OCTA technology, along with the practical applications of qualitative and quantitative analyses in ophthalmic corneal and retinal research.

## BACKGROUND AND METHODS

Optical coherence tomography (OCT) is a new non-contact, non-invasive optical imaging diagnostic technology developed in the early 1990 s. It uses the reflection difference of different tissues in the eye to the incident light beam, and compares the reflected beam with the reference beam through the low coherence optical interference measuring instrument to determine the delay time and reflection intensity of the reflected light, so as to analyze the structure and distance of different tissues, and display the cross section structure of the tissue by computer processing imaging[1]. OCT is an optical analogue of ultrasound, but its axial resolution depends on the coherence characteristics of the light source, up to 10  $\mu\text{m}$ , and the penetration depth is almost not limited by the transparent refractive medium in the eye. Therefore, it can observe both the anterior segment and the posterior segment of the eye. The morphological

structure has a good application prospect in the diagnosis, follow-up observation and treatment evaluation of intraocular diseases, especially retinal diseases [2, 3]. OCT angiography (OCTA) is a non-invasive vascular imaging technology based on OCT, which has the characteristics of non-invasive, high speed and high resolution. It can provide three-dimensional images of retinal and choroidal vascular structures to achieve quantitative and hierarchical detection of lesions [4, 5]. Compared with traditional dye angiography methods such as FFA and ICGA, OCTA has the advantage of being non-invasive and avoiding complications that may be caused by dye injection, such as allergic reactions or subcutaneous hematoma. OCTA examination is fast, usually completed within a few minutes, and has high-resolution imaging capabilities, allowing multiple repeated examinations in a short period of time, which is

convenient for continuous tracking of disease changes. By dynamically analyzing the changes of reflected light waves in the sample, OCTA can achieve excellent blood flow dynamic detection performance on the microvascular structure. This technique is based on the detection principle of flowing blood cells in fundus blood vessels, and repeats the coherent optical tomography of the same cross-section of the fundus. Through a special calculation method, obtain the signal of blood flow; based on this, the three-dimensional reconstruction of the vascular structure is performed, and the fundus vascular images are presented layer by layer in the form of coronal plane (En face) [6]. However, in the field of small animal science research, due to the large difference in eyeball size between small animals and humans, coupled with the different experimental requirements, the complexity of animal experiments, the diversity of scientific research tasks, and the short training time of scientific research instrument operators compared with clinical instrument operators, the lack of experience in the use of instruments and the replacement of personnel, these factors work together to lead to the fact that even under scientific and rigorous research conditions, scientific research results may still obtain less accurate OCT / OCTA results. In order to solve this problem, China Ophthalmic Imaging and Intelligent Medical Committee established an expert group on " Standard Operation Guide for Small Animal Optical Coherence Tomography and Optical Coherence Tomography Angiography. " It organized writing experts and ophthalmic imaging experts to study the application research literature of small animal ophthalmology, and held offline and online meetings based on the clinical research experience of OCT and OCTA. The first draft of the guide was written by the members of the writing

expert group. After the first draft was formed, the experts independently read and proposed amendments through e-mail and WeChat, and submitted them to the core members of the guide writing group respectively. The revision opinions were sorted out and discussed and summarized through WeChat, e-mail and online meetings. During the revision period, the guidelines fully accepted the suggestions and guidance of the participating experts, and finally reached the final draft of the guidelines. The guideline aims to summarize the technical principles, operation procedures and experimental precautions of OCT / OCTA in the anterior segment and retina of small animals. At the same time, the guideline also discusses the reference standards of quantitative indicators such as retina, cornea and microvessels of different animals under OCT / OCTA technology and the application of OCT / OCTA qualitative and quantitative analysis in ophthalmic cornea and retina research.

In 1991, Fujimoto and Davide Huang ( Casey Eye Institute, University of Health and Science, Oregon ) first proposed OCT technology [1]. In 1996, Zeiss first launched the clinical time-domain optical coherence tomography (OCT) system in ophthalmology. OCT has undergone the technical iteration of time-domain system, spectrum system and frequency scanning system. In 2016, the OCTA-based ophthalmic vascular microcirculation imaging system has been widely promoted. The vascular microcirculation imaging system is based on the OCT hardware system through algorithm upgrade and optimization to achieve contrast-free microvascular imaging, and gradually replace the clinical ophthalmic confocal fluorescence imaging system [1]. In the following, we introduce the small animal OCT and OCTA in detail.

## **OPTICAL COHERENCE TOMOGRAPHY SYSTEM**

### **Principle of operation**

OCT uses the near-infrared light beam of about 830 nm

band to pass through the transparent chambers and tissue layers of the eye at different speeds, and converts the reflected signals obtained at different positions into digital

signals. Through software processing, a non-invasive high-resolution cross-sectional image is generated[7]. Most commercial OCT devices usually use spectral domain technology to generate a chart (A-scan) of tissue reflectance and axial distance by irradiating the near-infrared narrow-band beam to the eye and interfering with the reference beam, and then mathematically processing. These devices can generate images similar to histological cross sections (B-scans), and some devices can also generate a three-dimensional structure data set (rectangular volume) of eye tissue by raster scanning [8, 9].

In mouse vision research, devices with fast acquisition rate and wide acquisition range are commonly used. Compared with clinical applications, ophthalmic research has various requirements for equipment, diverse research objects, low frequency of use, and limited research funds.

### **Process of operation**

First, anesthetise the experimental subjects. Taking the experimental sample of C57BL / 6 strain as an example, inject 1.25 % tribromoethanol intraperitoneally at a dose of 0.2 mL / 10 g. After anesthesia, add compound topiramate eye drops to the eyes of the experimental subjects for mydriasis.

Place the sample on the operating table, and align the eye

### **Application summary**

#### **1.1 Application of anterior segment of eye**

The change of corneal thickness is an important manifestation factor of corneal diseases. Accurate measurement of corneal thickness can be applied to the diagnosis of diseases such as dry eye, keratitis and glaucoma[10].OCT imaging equipment can quickly and non-contact obtain high-resolution tomography of the cornea, providing the possibility for accurate measurement of corneal thickness [11]

Small animal OCT needs to achieve the integration of anterior segment and retinal function as much as possible under the conditions of technical permission, and is compatible with a variety of animal imaging. Ideally, a high signal-to-noise ratio image should be obtained in a single exposure, and the exposure time should be short enough to reduce motion artifacts caused by eye movement, heartbeat, respiration, and mouse movement. However, since the data generated by the currently available commercial equipment in a single short exposure is relatively noisy, the image quality can be improved by obtaining multiple exposures, followed by image alignment and average processing. Digital processing is further used to adjust direction, compensate for uneven illumination, sharpen, and optimize brightness and contrast to improve image appearance.

of the sample with the lens for Liner mode scanning. By changing the scanning lens, adjusting the scanning position and distance, the anterior segment or retinal tomography image is completely and clearly presented on the display. Perform the Volume mode scanning to obtain a complete coronal plane (En-face). Click to save and output to obtain the gray-scale cross-sectional images of En-face and each vertical section on the surface. The measurement software provided by the device can be used to measure any line segment, angle and other parameters on the anterior segment or retinal image.

Cornea is a transparent and slightly prominent discoid membrane at the front end of the animal eyeball. It is thin in the middle and thick in the edge, without any blood vessels. Severe keratitis can induce neovascularization [12, 13]. Taking C57BL / 6 mice as an example, in order to collect clear and accurate corneal OCT images, small animals need to be deeply anesthetized before collection and fixed on the supporting mouse platform smoothly.

Before shooting, confirm that there is no occlusion between the cornea and the lens (such as mouse beard), and the corneal surface is clean and free of debris. If there are tears or other liquids on the surface of the cornea, it should be wiped in time to keep clean. When the corneal OCT tomographic image appears in the software image, it is necessary to adjust the eye orientation of the mouse by adjusting the supporting

mouse platform, so that the pupil position in the En-face image is facing the lens, and the pupil position of the tomographic image is in the middle position. Move the mouse platform forward and backward, so that the cornea in the tomographic image is at the focus position. The cornea can clearly see the structure of each layer at the focus position, as shown in Fig.1.

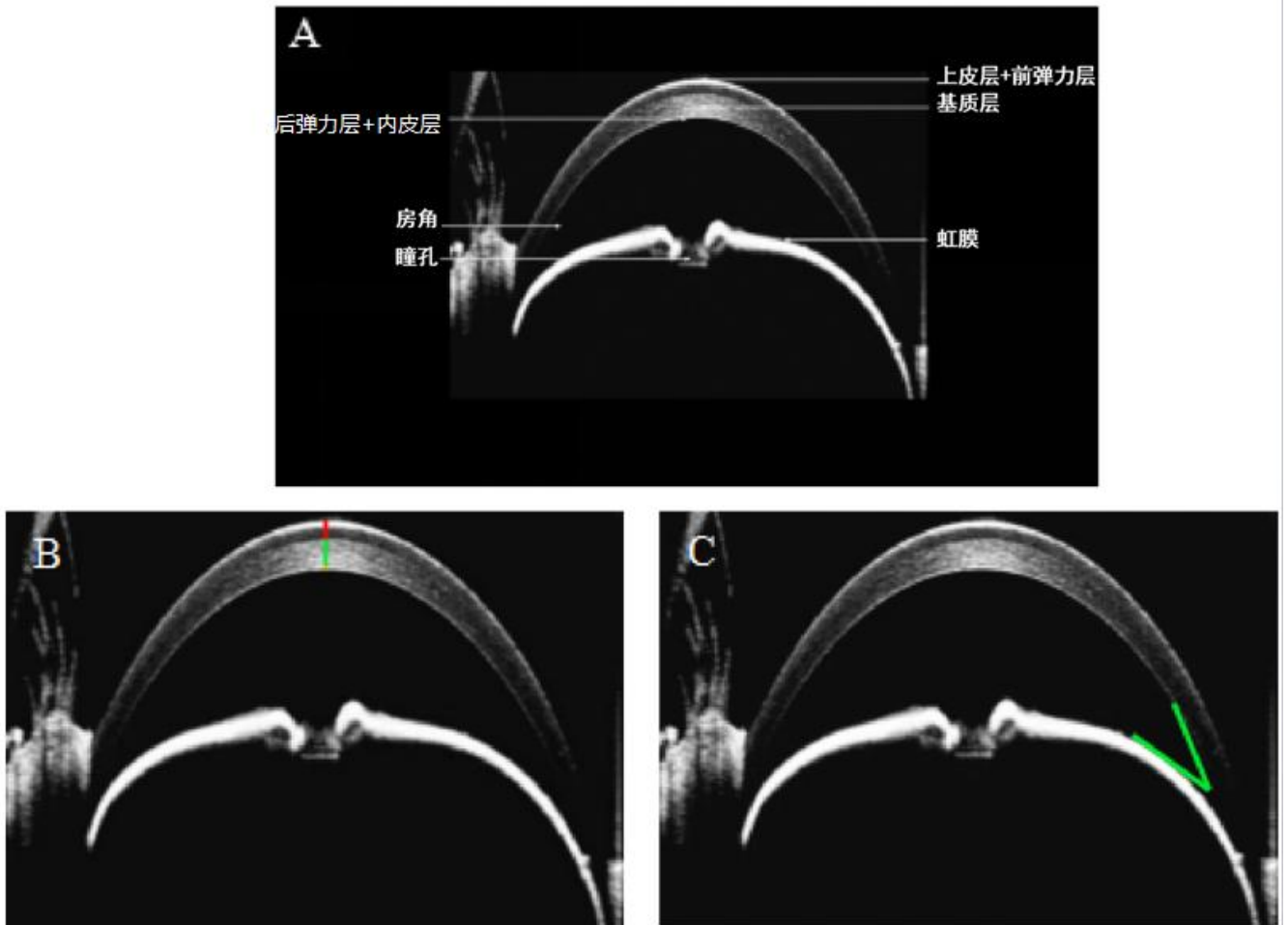


**Figure.1** Normal C57BL / 6 mouse corneal OCT standard image

A: Hierarchical labeling of corneal OCT images of normal C57BL/6 mice; B: Schematic diagram of corneal OCT thickness measurement in normal C57BL/6 mice; C: Schematic representation of corneal OCT Angle measurement of C57BL/6 mice (Angle 30°).

Corneal OCT mainly evaluates the thickness of the three layers of epithelium + anterior elastic layer, stroma layer and posterior elastic layer + endodermis. It is recommended to use point-to-point measurement or point-to-point overall corneal thickness measurement (i.e., single-point or multi-point thickness measurement at a

specific position of the cornea). The operator can select the key positions on the cornea, such as the central, peripheral or other specific points of the cornea, for accurate thickness measurement). The thickness stratification is shown in Figure 1A. Corneal OCT measurements of adult C57BL / 6 mice are shown in

Table 1. The thickness of the epithelial layer + anterior elastic layer is  $45.70 \pm 1.74\mu\text{m}$ , the thickness of the stroma layer is  $68.60 \pm 1.79\mu\text{m}$ , and the thickness of the

posterior elastic layer + endodermis is  $7.10 \pm 0.43\mu\text{m}$ . The corneal OCT angle measurement diagram is shown in Fig.1C, and the angle of the chamber angle is  $30^\circ$ .

**Table 1. Measurement of corneal OCT thickness in C57BL / 6 mice**

Name	Thickness ( $\mu\text{m}$ )
Epithelial layer + anterior elastic layer	$45.70 \pm 1.74$
Stroma layer	$68.60 \pm 1.79$
Posterior elastic layer + endodermis	$7.10 \pm 0.43$

**Table 2. Table of central corneal OCT thickness measurements for different animals**

Species of animals	Thickness ( $\mu\text{m}$ )
SD rat	$154.10 \pm 9.00$
New Zealand white rabbits	$11.72 \pm 0.65$
Rhesus monkey	$489.17 \pm 17.82$
Pig	$977.45 \pm 34.15$

The standard corneal OCT images of different species of animals (zebrafish, C57BL/6 mice, SD rats, guinea pigs,

New Zealand white rabbits and pigs) are shown in Figure 2.

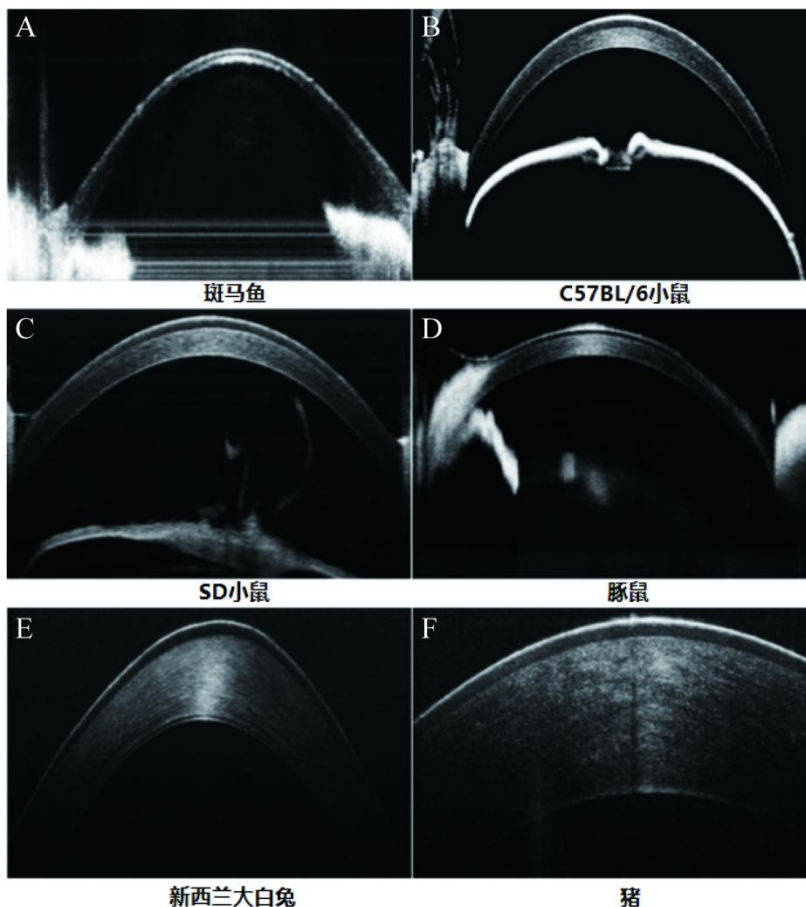


**Figure 2.** Standard corneal OCT images of different animal species

A: Zebrafish; B: C57BL/6 mice; C: SD rats; D: Guinea pigs; E: New Zealand white rabbits; F: Pigs.

Irregular images taken:

The main manifestation is unclear corneal image

structure. The reason may be that the animal is not well anesthetized. During the image acquisition process, the animal jitters to form a focus shift, resulting in defocus, or the corneal surface is not clean enough to cause poor imaging quality. Non-standard images are shown in

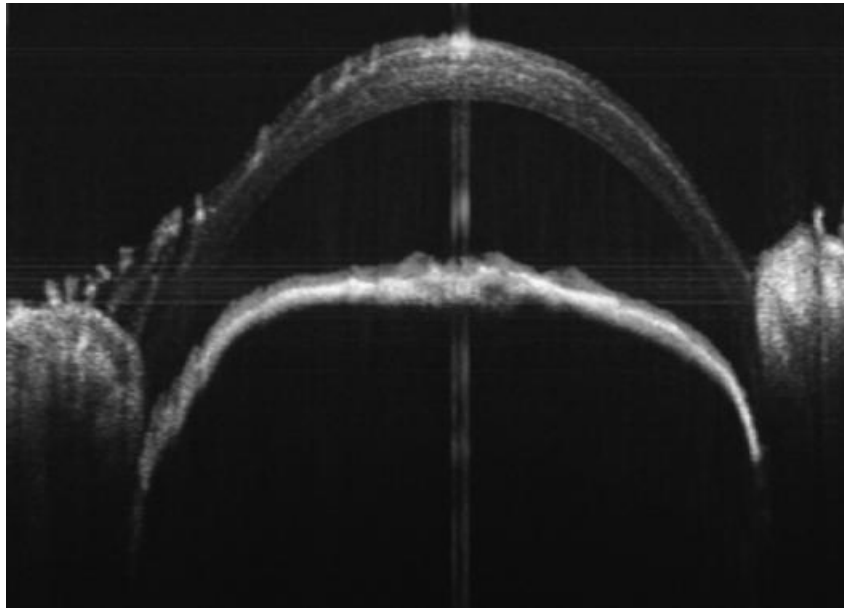


**Figure 3.** Non-standard corneal OCT images

## 1.2 Applications in the axis oculi

Axial length measurement is an important technique in the field of ophthalmology, which is used to evaluate the length of the eyeball, so as to help diagnose and treat various ocular diseases, especially myopia, hyperopia and other refractive errors [10, 14]. The earliest methods of axial measurement include the use of A-scan ultrasound biometry [15]. With the development of science and technology, axial measurement technology is also in constant progress and evolution. Small animal OCT technology enables researchers to non-invasively observe

### 1.2.1 Principle of operation

OCT uses the measured delay of light pulse scattering and propagation inside the sample to form a high-resolution image through processing to analyze the

### 1.2.2 Operation processes

Before starting data collection, animals need to be prepared to ensure stable experimental conditions and animal safety. The following are some key steps (taking OPTOPROBE brand equipment, model ISOCT as an example):

Figure 3.

Solution: Note that the degree of anesthesia of the animal is deep anesthesia, change the anesthetic if necessary, and use a wet cotton swab to gently wipe the corneal surface.

and measure the structure of small animal eyeballs, including cornea, lens, vitreous and so on [16, 17]. This is of great significance for understanding the biological characteristics, development process and structural changes related to eye diseases [18].

In summary, small animal OCT technology has important application value in ophthalmology research and medicine, which can provide valuable information and support for axial biology, eye disease research and new technology development.

internal microstructure of the sample without physical contact, and can quickly and clearly obtain non-invasive two-dimensional and three-dimensional images.

(1) Preparation: Prepare the laboratory environment to ensure that the operation area is clean and tidy, and avoid possible light pollution and stray light affecting the imaging quality. Check and calibrate the OCT equipment to ensure that the equipment is working properly.

Preparation of experimental animals, including the selection of appropriate small animal models (such as mice or rats) and preparation of animal anesthesia.

(2) Animal anesthesia and fixation: According to the type and weight of animals, choose the appropriate method for anesthesia. Taking the experimental sample of C57BL / 6 strain as an example, inject 1.25 % tribromoethanol intraperitoneally at a dose of 0.2mL/10g[19]. Anesthesia needs to be carried out under the guidance of professionals to avoid animal injury. Fix the animal on the supporting platform to prevent jitter during operation. The shooting time should not be too long. During the shooting process, normal saline or sodium hyaluronate eye drops can be used to keep the animal 's ocular surface wet, so as to avoid the animal 's corneal whitening caused by too long shooting time and affect the anterior segment shooting.

(3) Scanning parameter setting: Set appropriate scanning parameters, including scanning speed and range, for specific small animal models and imaging requirements. Eye positioning and focusing: click on the ' preview ' button in the software, use the image preview function of the OCT device to locate and focus on the eye area, usually the center of the eye axis.

(4) Image acquisition: Click the ' OCT ' button to start scanning, and the beam will gradually scan the entire

axial area to obtain a series of B-Scan images.

(5) Data storage: Click the ' SAVE ' button to save the acquired image data in a computer or data storage device, ensure data integrity and security.

(6) Data processing and analysis: Images were measured using professional image processing software to obtain axial length and parameters of other structures.

(7) Result presentation: The processed data and images are used for research reports, papers or demonstrations.

(8) Cleaning and maintenance: After the operation is completed, the equipment and operation area should be cleaned in time to maintain the normal state of the equipment. Maintain OCT equipment, including calibration and maintenance, if necessary. Operators should strictly follow the safety procedures when performing small animal axial OCT operations to ensure the well-being of animals and laboratory safety. The specific details and steps in the operation process may vary depending on the purpose of the experiment, the type of equipment and the operator 's experience.

Shoot the OCT image that meets the requirements of the specification: the image is clearly focused, no eyelashes or eyelid occlusion, and the entire eyeball structure can be completely displayed, so that the axial length can be measured according to the image (Fig.4A ).

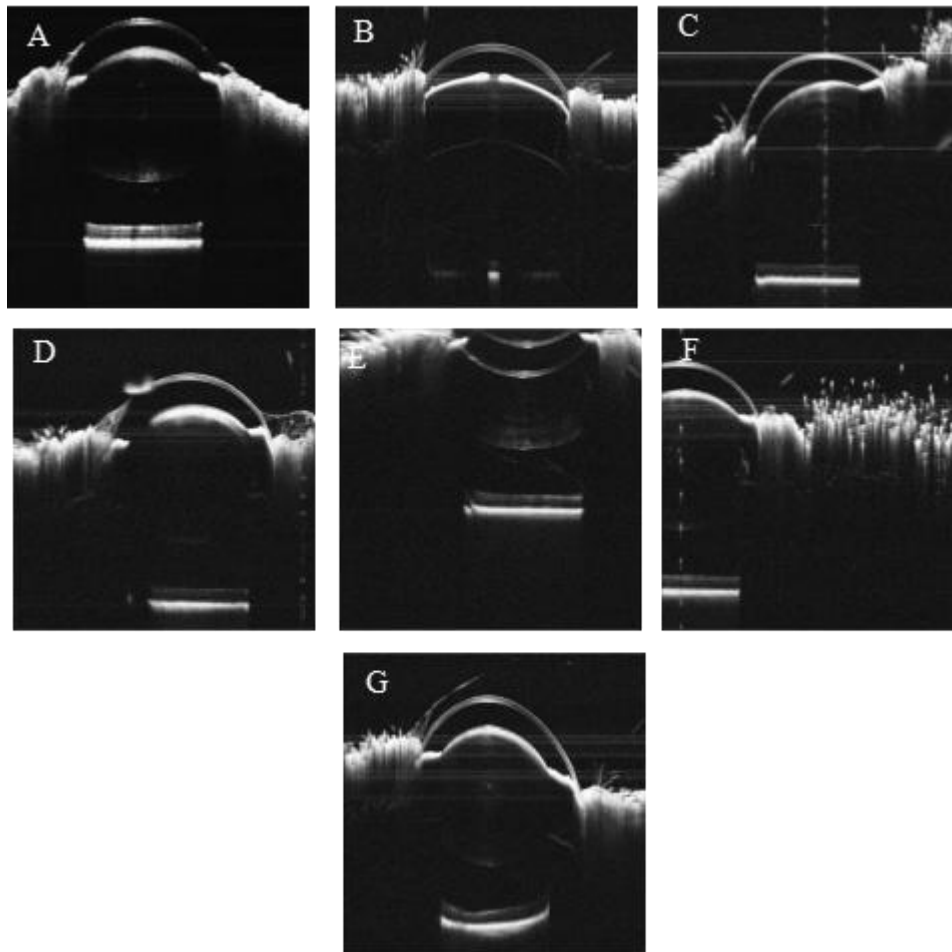


**Figure 4.** Images of axial length obtained with ISOCT

A: Standard image of the axial length of a normal C57BL/6 mouse; B: non-standard images due to incomplete mydriasis or without mydriasis; C: non-standard image shooting caused by eyeball orientation not facing the lens; D: irregular images caused by occlusion; E: non-standard image shooting caused by not reaching the focus position; F: non-standard image due to eye not in the scanning area; G: Irregular images caused by mydriasis or other fluids not being cleaned.

**Table 3. Axial length values measured by OCT in different animals**

Species of animals	Axial length of eye (mm)
C57BL/6mice	2.98 ± 0.034
Adult SD rats	6.91 ± 0.44
New Zealand white rabbits	14.63 ± 0.19
Rhesus monkeys	20.32 ± 0.84
Guinea pigs	about 7.30 at birth
	about 8.30 in 30 days
	Up to 9.60 at 1 year of age

Non-standard axial OCT images taken:

1.The pupil is not dilated and the image fail to cover the fundus (Fig.4B).

Solution: Use mydriatic eye drops to fully disperse the

pupil of the animal.

2.The eyeball orientation was not directly facing the lens (Fig.4C).

Solution: It is recommended to use the cross scanning

mode for alignment during acquisition.

3. Beard or eyelash occlusion in front of the eye (Fig.4D).

Solution: Use a wet cotton swab to gently wipe or use a cotton swab dipped in a gel to wipe the eyelashes and beard to one side.

4. Not reach the focus position (Fig.4E).

Solution: move the small animal test bench away from the lens and adjust to the focus position.

5. The eyeball is not in the scanning area (Fig.4F).

### 1.3. Applications in the retina

The retina is a nerve ending tissue and belongs to a part of the central nervous system. From the histological point of view, from outside to inside are retinal pigment epithelium, photoreceptor layer, outer membrane, outer nuclear layer, outer plexiform layer, inner nuclear layer, inner plexiform layer, ganglion cell layer, nerve fiber layer and inner limiting membrane [20, 21]. OCT uses depth-resolved analysis of the spectral information contained in the backscattered light returned by the sample to distinguish different cell types. It can not only visualize and track the complex dynamic changes in the engineered tissue, but also study the longitudinal development of the engineered tissue and cell dynamics, such as migration, proliferation, separation, and cell-material interactions [22]. The diameter of the flat mouse retina is about 5 mm, the diameter of the normal retina is about 20 mm, and the diameter of the human retina is about 40 mm [18]. Taking C57BL / 6 mice as an example, in order to collect clear and accurate retinal OCT images, small animals need to be deeply anesthetized before collection, and they should be stably fixed on the supporting mouse platform. Before shooting, it is necessary to confirm that there is no other debris between the eyeball and the lens (such as mouse beard, etc.). After cleaning, the mouse eyeball is in contact with the lens, and the mouse eyeball orientation is adjusted by adjusting the supporting mouse platform, so that the optic disc in the En-face image is located in the center of the field of vision. Move the mouse platform forward and backward, so that the retina in the tomographic image is at the focus

Solution: by moving the small animal experiment platform to move the X-axis, the image is moved to the display area.

6. Eye surface mydriasis or other liquid is not clean (Fig. 4G).

Solution: use wet cotton swab to wipe the ocular surface liquid clean; note that the degree of animal anesthesia is deep anesthesia, change the anesthetic if necessary, and use a wet cotton swab to gently wipe the corneal surface.

position, and the structure of each layer of the retina can be clearly seen. The image details are shown in Fig. 5A, from which the layers and organizational structure can be clearly observed.

For retinal OCT, it is recommended to use quantitative analysis software (OCT Image Analysis) or other software to delineate the area that you want to analyze, and perform automatic stratification measurement of the main structure of the retina, as shown in Figure 5B and Table 4. Manual correction is recommended for areas where the fault structure is not obvious due to disease. The measurement range of retinal OCT thickness in normal mice is shown in Table 4 (for reference). For example, the thickness of nerve fiber layer is  $18.40 \pm 1.59 \mu\text{m}$ , that of ganglion cell layer-inner plexiform layer is  $49.30 \pm 2.12 \mu\text{m}$ , the inner nuclear layer is  $26.20 \pm 1.09 \mu\text{m}$ , the outer plexiform layer is  $14.20 \pm 1.02 \mu\text{m}$ , the outer nuclear layer is  $56.10 \pm 1.95 \mu\text{m}$ , the outer membrane is  $12.10 \pm 1.06 \mu\text{m}$ , and the photoreceptor cell layer is  $40.60 \pm 3.14 \mu\text{m}$ , the pigment epithelium is  $13.00 \pm 2.81 \mu\text{m}$ .

Nonstandard images:

During the data collection process, the animal is not anesthetized well, and the movement form a focus shift, resulting in a loss of focus in the regional position. The non-standard images of retinal OCT acquisition are shown in Figure 5C. Solution: Pay attention to the degree of animal anesthesia for deep anesthesia or replacement of anesthetics.

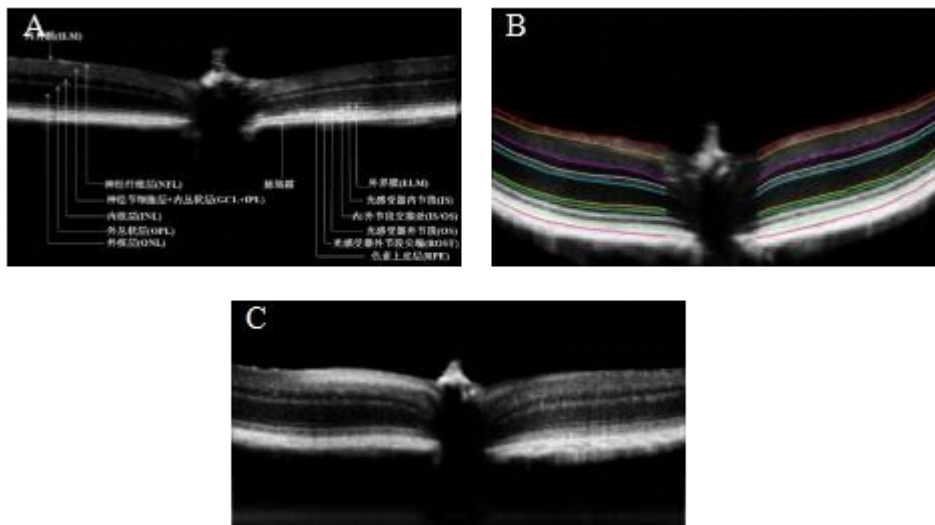


**Figure.5** Pictures of retinal OCT collected by ISOCT instrument

A: Presentation of retinal OCT layers in normal C57BL/6 mice; B: Retinal OCT thickness measurement pattern of normal C57BL/6 mice; C: Nonstandard retinal OCT images.

**Table 4. Retinal OCT thickness measurements in normal C57BL/6 mice**

Name	Thickness ( $\mu\text{m}$ )
Nerve fiber layer	$18.40 \pm 1.59$
Ganglion cell layer-inner plexiform layer	$49.30 \pm 2.12$
Inner nuclear layer	$26.20 \pm 1.09$
Outer plexiform layer	$14.20 \pm 1.02$
Outer nuclear layer	$56.10 \pm 1.95$
Membrana limitans externa	$12.10 \pm 1.06$
Photoreceptor layer	$40.60 \pm 3.14$
Pigment epithelium layer	$13.00 \pm 2.81$

**Table 5. Retinal OCT thickness measurements in normal 6-week-old SD rats**

Name	Thickness ( $\mu\text{m}$ )
Full thickness	$190.79 \pm 11.70$
Inner limiting membrane to inner plexiform layer of retina	$69.13 \pm 4.25$
Inner nuclear layer	$26.69 \pm 6.90$
Outer nuclear layer to pigment epithelium layer	$9.13 \pm 12.48$

The retinal OCT standard images of different species of animals (zebrafish, C57BL / 6 mice, SD rats, BN rats, guinea pigs, New Zealand white rabbits, pigs and rhesus

monkeys) are shown in Figure 6, which can clearly observe the tissue structure of each layer of the retina.

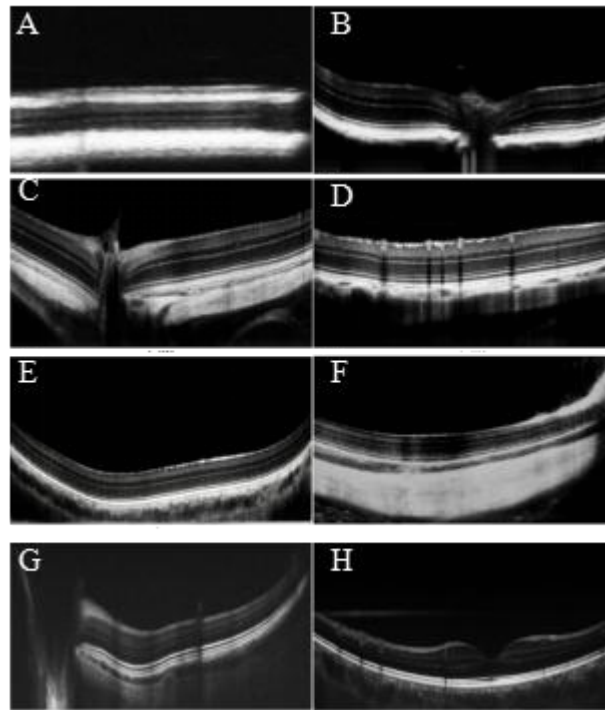


**Figure 6.** Standardized retinal OCT images of different animal species

A: zebrafish; B: C57BL/6 mice; C: SD rats; D: BN rats; E: guinea pigs; F: New Zealand white rabbits; G: pigs; H: rhesus monkeys.

## PRINCIPLE OF OPTICAL COHERENCE TOMOGRAPHY ANGIOGRAPHY

### Principle

The technical principle of optical coherence tomography angiography (OCTA) is mainly based on the concept that in the static eyeball, the only moving structure of the fundus is the blood cells flowing in the blood vessels[23, 24]. The same cross section of the sample is repeatedly scanned (B-scan) using a near-infrared beam in the 1060 nm band. Through special calculation methods, such as the decorrelation of signal amplitude, the comparison of

**Operating procedure**

First, anesthetize the experimental subjects. Take the experimental sample of C57BL / 6 strain as an example, inject 1.25 % tribromoethanol intraperitoneally at a dose of 0.2 mL/10g. After anesthesia, drip compound tropicamide into the eyes of the experimental subjects for mydriasis.

static and active structures is generated to obtain blood flow signals. Based on this, the three-dimensional reconstruction of the vascular structure is performed and usually presented layer by layer in the form of coronal plane (C-scan or En face), which can obtain the lesion range of the anterior segment and fundus and evaluate the hemodynamics of the anterior segment blood vessels and retinal blood vessels[25, 26].

Place the sample on the operating table, and align the eye of the sample to the lens for Liner and Preview mode scanning. By changing the scanning lens and adjusting the scanning position and distance, a clear and complete anterior segment or retinal fault and En-face image are presented on the display. Then perform the OCTA mode

scanning to obtain the three-dimensional original data of the anterior segment or retina. The software provided by the device can be used to reconstruct the three-dimensional blood vessels of the original data, and the

## 2.1 Application of anterior segment

The iris is a visible colored part of the eye, in which the pupil can adjust the amount of light in the eye by changing the size. The iris has a rich blood supply, and trauma can easily lead to intraocular hemorrhage [27, 28]. Brown iris contains more pigment, blue iris contains less pigment. Taking C57BL / 6 mice as an example, in order to obtain clear and non-impurity iris OCTA images, small animals need to be deeply anesthetized before image acquisition, and then fix their heads on the head fixator. Before shooting, it is necessary to confirm that there is no other debris between the cornea and the lens (such as mouse beard). By adjusting the supporting mouse platform to adjust the mouse eye orientation, the pupil position of the iris in the En-face image is in the center of

En-face can be presented layer by layer to analyze and evaluate the blood vessels of the anterior segment and the retinal layers.

the visual field. Move the mouse platform forward and backward, so that the iris in the tomographic image can obtain a clear image at the focus position. The details of the image are shown in Figure 7A, from which you can clearly observe the layer and clear network direction. The arteries of the iris are located in the stroma and radiate from the edge to the center of the iris, providing blood supply to the iris. There is a thick vascular ring in the iris root and anterior ciliary, which is called the iris artery ring. The iris big ring emits radial branches from the periphery of the iris to the center, and emits many small branches at the pupil contraction wheel and changes the direction to form a small ring of the iris artery.

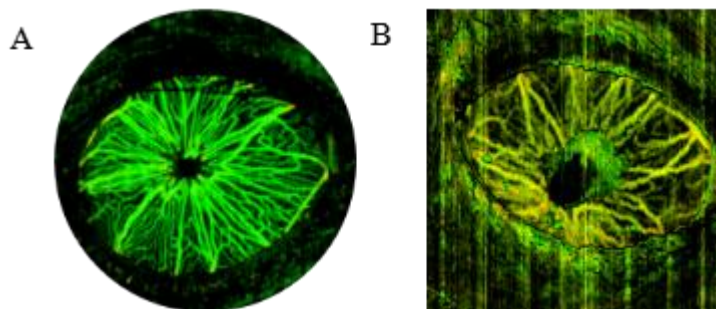


**Figure 7.** Canonical and noncanonical images of iris OCTA in normal C57BL/6 mice  
A: Standard OCTA diagram of iris; B: Non-standard OCTA diagram of iris.

Nonstandard images:

Due to the loss of focus caused by improper anesthesia or fixation, there are too many mixed signals in the iris OCTA image, which leads to inaccurate data analysis, as

## 2.2 Application in the retina

The retina of animal fundus contains two kinds of light-sensitive cells (rod-shaped cells and cone-shaped cells). Rod-shaped cells are highly sensitive to dark light and can provide good peripheral vision and motion. Conical cells are sensitive to sunlight and can provide good sense

shown in Fig.7B.

Solution: Pay attention to the degree of animal anesthesia for deep anesthesia or replacement of anesthetics, and tighten the mouse fixator.

of shape and color perception [20, 21]. There are differences in the retinal vascular system between humans and rodents. For example, there is no foveal avascular zone (FAZ) due to the absence of fovea in rodents. In addition, the number of vascular plexuses in

the retina is not the same, and these vascular plexuses are not entirely located in the same layer of retina. In different regions of the human retina, we can find 1-4 vascular plexuses. In rodents, except for the outermost retina, there are only two vascular plexuses. The vascular structure of the retina is organized into three connected nerve plexuses, which are superficial vascular plexus, intermediate capillary plexus and deep capillary plexus [29, 30]. In order to collect clear and accurate retinal OCT images, and to perceive the color of normal C57BL/6 mice, the small animals should be deeply anesthetized before collecting the images, and they should be stably

fixed on the supporting mouse platform. Before shooting, it is necessary to confirm that there is no other debris between the eyeball and the lens (such as mouse beard) to avoid signal loss. Adjust the eye orientation of the mouse to make the optic disc position in the En-face image in the center of the visual field. Move the mouse platform forward and backward, so that the tomographic image is moved to the focus, and the optic disc position is in the middle position, and the structure of each layer of retina can be clearly seen. The details of the image are shown in Figure 8.

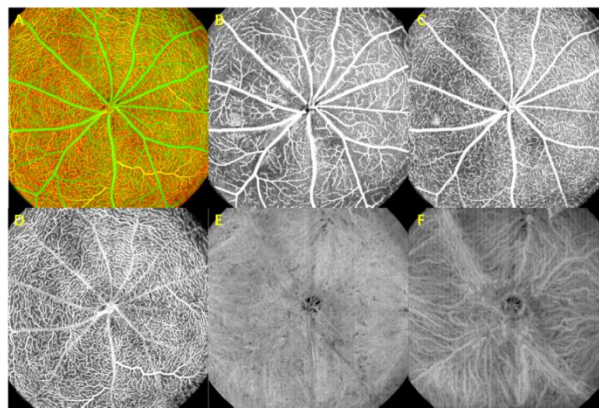


**Figure 8.** OCTA images of the retina of normal C57BL/6 mice

A: retina - color map; B: nerve fiber layer - grayscale image; C: inner plexiform layer - grayscale image; D: outer plexiform layer - grayscale image; E: superficial choroids-grayscale image; F: Deep choroid -grayscale map.

Non-standard images:

Partial out-of-focus resulted in unclear retinal OCTA, and

the nonstandard images are shown in Fig.9.

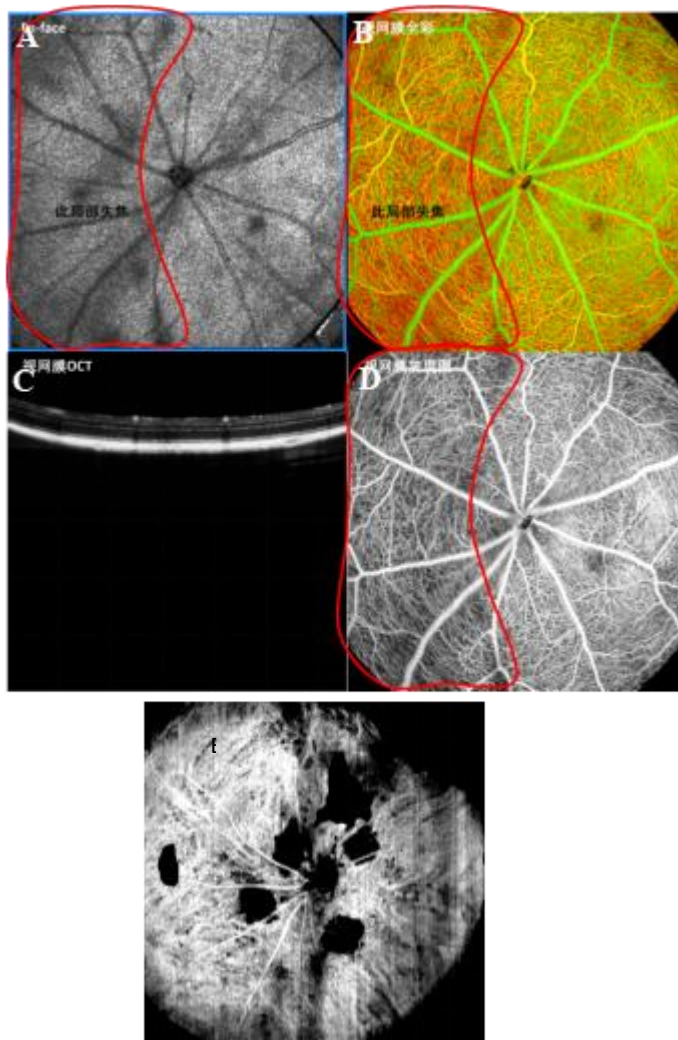


**Figure 9.** Non-standard OCTA images of retina and choroid

A: En-face image of retinal OCT; B: OCTA color map of retina; C: retinal OCT tomography; D: OCTA grayscale image; E: Choroidal OCTA irregularity map. The image in the red box in the figure is not imaged clearly.

The application of retinal vein occlusion microvascular abnormality model: Taking C57BL/6 mouse retinal vein occlusion microvascular as an example, see Fig.10. The position indicated by the red arrow on the 5-day color map shows the state of filling the blood vessels near the optic disc, and the blood vessels away from the optic disc

are in a state of vascular obstruction (Fig.10A). The location indicated by the red arrow on the color map of the 12-day occlusion shows that the blood vessels near the optic disc are in an ischemic state, and the blood vessels away from the optic disc disappear (Figure 10B).

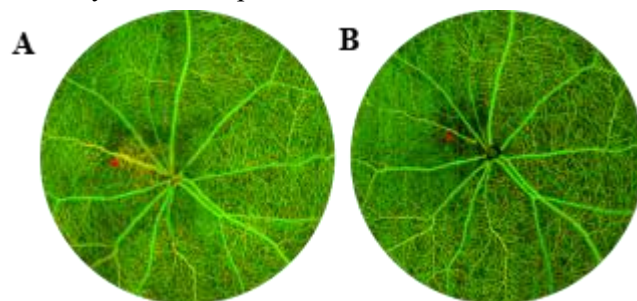


**Figure 10.** Microvascular Changes in retinal vein occlusion in C57BL/6 mice

A: OCTA image of occlusion for 5 days; B: OCTA image of occlusion for 12 days.

### 2.3 Application in the choroid

The choroid is a dark brown vascular layer, located between the sclera and the retina, rich in blood vessels and pigment granules, and provides nutrients for the retina [31, 32]. In order to collect clear and accurate choroidal OCT images, fix the small animals stably on the supporting mouse platform to avoid jitter, and confirm that there is no other debris between the eyeball and the lens. Move the mouse platform back and forth to move the tomographic image to the focus, and the optic

disc is located in the middle position, and the choroidal structure could be clearly seen. The normal choroidal OCTA image shows as E and F in Figure 11, E is the grayscale image of the superficial choroid, and F is the grayscale image of the deep choroid.

The standard OCTA images of the retina and choroid of SD rats are shown in Fig.11, which can clearly observe the layer and tissue structure.

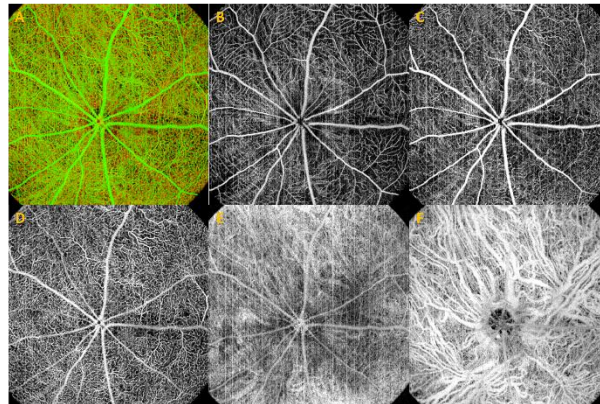


**Figure 11.** OCTA of retina and choroid in SD rats

A: retina - color map; B: nerve fiber layer - gray scale; C: inner plexiform layer - grayscale image; D: outer plexiform layer - grayscale image; E: superficial choroids-grayscale image; F: Deep choroid -grayscale map.

Non-standard images:

Choroidal OCTA is not clear due to foreign bodies on the cornea. The non-standard images are shown in Fig.12. The images are unclear or missing a lot of information.

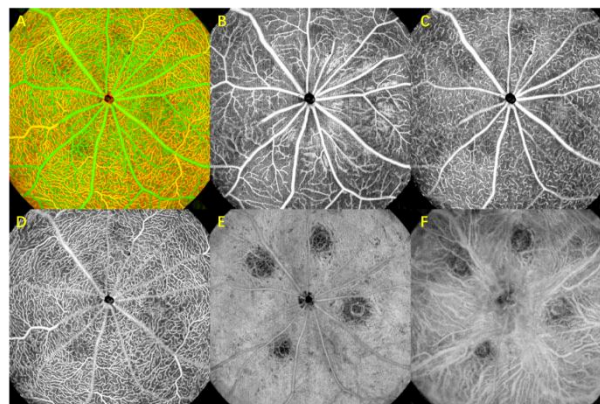


**Figure 12.** OCTA images of the retina and choroid in C57BL/6 mice, a model of choroidal neovascularization

A: retina - color map; B: nerve fiber layer - gray scale; C: inner plexiform layer - grayscale image; D: outer plexiform layer - grayscale image; E: superficial choroids-grayscale image; F: Deep choroid -grayscale map.

## MATTERS NEEDING ATTENTION

The anesthetic effect of animals, body position and other factors will directly affect the data collection and post-processing. Therefore, in order to obtain accurate corneal and retinal OCT / OCTA data, the following points should be noted during measurement:

(1) Anesthesia: Ensure that small animals are properly anesthetized before OCT/OCTA acquisition and provide a comfortable environment. Attention should be paid to the type, dose and action time of anesthetics to ensure the welfare and safety of animals. It is recommended to use a configured 1.25 % afodin (tribromoethanol) for anesthesia.

(2) Pupil dilation: Use the pupil dilation agent to expand the pupil of small animals to ensure sufficient light entering the eyeball, so as to obtain clear tomographic and microvascular images. It is recommended to use compound tobecalamine eye drops for mydriasis for 1 minute.

(3) Fixation: Ensure that the eyeballs of small animals remain stable during the acquisition process to reduce the impact of eye movement on image quality. Use appropriate fixation devices or brackets to fix the head of small animals. It is recommended to use a specially customized mouse platform with a bite stick.

(4) Temperature and humidity control: Maintain appropriate temperature and humidity conditions to ensure the stability of the physiological state of small

## APPLICATION OF SCIENTIFIC RESEARCH PRACTICE

OCT / OCTA is a technology that uses the interference principle of low coherent light to obtain the internal structure information of biological tissues. It can provide high-resolution, non-invasive and real-time tomographic images and has been widely used in medical and biological fields. In corneal research, OCT / OCTA technology can be used to observe the thickness, shape and curvature of the cornea in mice, so as to evaluate and monitor various corneal disease models, such as corneal transplantation, corneal defect or corneal infection. It can

animals. Too high or too low temperature may affect the image quality [33, 34]. It is recommended to add a heating pad with a constant temperature of 37 °C.

(5) Tear film status: After anesthesia, the mice could not close their eyes autonomously, and the tear film evaporate. The lack of water in the cornea leads to the disorder of lens circulation, causing lens opacity[35]. Artificial drip of artificial tears will affect the entire optical path acquisition, resulting in local shadows in the study area, which will directly affect the acquisition of tomographic imaging and microvascular signals. It is recommended to gently wipe with a cotton swab dipped in normal saline in one direction before collecting anterior segment OCT/OCTA to remove residual mydriatic fluid or artificial tears.

(6) Collection adjustment: Because the position of the anesthetized mice cannot be subjectively moved, the deviation of the cornea will directly affect the accuracy of the thickness measurement.

(7) Layering adjustment: Because of the disease, the layered structure of cornea and retina is not clear. It is recommended to use the cross-scan mode to evaluate the transverse and longitudinal direction of the cornea, and then perform different modes of scanning according to the specific situation; manual subjective correction is recommended for areas where the fault structure is not obvious due to disease.

also be used to detect changes in corneal function in mice, such as corneal sensory nerve density or corneal endothelial cell count. In retinal research, OCT / OCTA technology can be used to observe the thickness, morphology, layer and blood flow of the retina in mice, so as to evaluate and monitor various retinal disease models, such as macular degeneration[36], diabetic retinopathy [37] or retinal ischemia-reperfusion[38]. OCT / OCTA technology has played an important role in the study of mouse ophthalmology, providing scientists with

more information on the structure and function of mouse intraocular tissues, and providing a valuable tool for the establishment, evaluation and monitoring of mouse eye disease models.

Compared with traditional fundus examination and fundus photography, OCT / OCTA technology can provide detailed information and structure of each layer of the retina, such as nerve fiber layer, retinal ganglion cell layer and vascular layer. OCT / OCTA can be used for early screening, diagnosis and treatment evaluation of

## **LIMITATIONS**

OCT technology has shown great potential in the application of small animal ophthalmology, but there are also some limitations. The following is an analysis of these limitations:

(1) Differences in eyeball size and anatomical structure: Small animals (such as mice and rats) have smaller eyeball size, shorter axial length, and smaller pupils. These anatomical differences make OCT imaging challenging. Since the size of the mouse eye is about 1 / 8 of that of humans, but its numerical aperture (NA) is more than twice that of humans, the effect of optical aberrations on image quality increases with the increase of NA, which hinders high-resolution imaging in mice. Therefore, it is necessary to use dedicated small animal OCT equipment, and may need to introduce an adaptive optical system to correct aberrations to improve imaging quality.

(2) Imaging depth limitation: The imaging depth of OCT technology is affected by the light source penetration and tissue scattering characteristics. For small animals, because their eyeballs are small and the internal tissue may be dense, this may limit the depth of OCT imaging. This may affect the observation and diagnosis of the deep structure of the fundus of small animals.

(3) Difficulty of image interpretation and diagnosis: OCT images provide cross-sectional information of retina and

## **CONCLUSIONS AND PROSPECTS**

The standardized use of OCT and OCTA in small animal

retinal diseases, helping doctors or researchers to observe and evaluate the structure and function of retinal blood vessels. OCT / OCTA uses the principle of light wave interference to generate high-resolution in vivo tissue images by measuring the time and amplitude of reflected light, providing detailed structural information for doctors or researchers, and providing a more comprehensive and accurate diagnostic basis for related animal experiments.

other tissues, but the interpretation and diagnosis of these images require certain professional knowledge and experience. For small animals, due to their anatomical structure and physiological characteristics are different from humans, more professional knowledge and skills may be needed to accurately interpret OCT images and make correct diagnosis.

(4) Cost and technical requirements: OCT technology requires high-precision optical systems and complex image processing algorithms, which leads to higher equipment costs. In addition, the operation and maintenance of OCT technology also requires a certain technical level and professional knowledge. For small animal research, this may increase the technical threshold and cost of its application.

In summary, the limitations of OCT technology in small animal applications mainly include eye size and anatomical structure differences, imaging depth limitations, image interpretation and diagnostic difficulties, as well as cost and technical requirements. However, with the continuous advancement of technology and the development of special equipment, these limitations are expected to be gradually overcome, thus promoting the wider application of OCT technology in small animal scientific research.

ophthalmology is of great significance in research and

practice. Using standardized OCT and OCTA data acquisition methods and parameter settings can ensure that the data obtained by different research units are comparable. This helps to promote data sharing and comparison between different studies and improve the reliability and reproducibility of scientific research results. The use of standardized acquisition methods can reduce the variability of experimental operations, thereby improving the consistency and stability of images. This helps to obtain accurate and reliable results and reduce errors and deviations. Normalization can also make it easier for researchers to interpret and analyze OCT and OCTA images. Consistent data collection methods help to reduce interference factors and make the results easier to understand and explain. Standardization can also improve the reliability and trust of the research. When the data collection and processing methods are consistent, the research results will be more convincing and help to

enhance the scientific value of the research. In the study of eye diseases in different animal models, standardized collection methods can make it easier for researchers to compare eye changes between different models. This helps to diagnose the disease more accurately and understand the similarities and differences between different models. In drug development and treatment monitoring, standardized OCT and OCTA methods can more accurately evaluate drug efficacy and therapeutic effect, and improve the credibility of research results. Standardization can simplify the training process and make it easier for new operators to master the operation skills and processes of OCT and OCTA.

In summary, standardized animal ophthalmic OCT and OCTA data acquisition methods and operating procedures help to improve the consistency, reliability and comparability of data, thus promoting the progress of ophthalmic research and clinical practice.

## ACKNOWLEDGEMENTS

### Expert Group Members

#### Leading authors

Yi Shao	Shanghai General Hospital of Shanghai Jiao Tong University School of Medicine
Jian Ma	Zhejiang University, Eye Center of Second Affiliated Hospital, School of Medicine
Zhao-Yang Wang	Beijing Tongren Hospital, Capital Medical University
Gang Tan	The First Affiliated Hospital of University of South China
Mu Qin	Affiliated Hospital of XiangNan College
Hong Zhang	The First Affiliated Hospital of Harbin Medical University
Yan-Yan Zhang	Ningbo Eye Hospital
Yi-Xin Wang	Affiliated Hospital of XiangNan College
Wei Chi	Shenzhen Eye Hospital, Shenzhen Eye Disease Prevention and Treatment Institute
Xin-Yue Zhu	Shanghai General Hospital of Shanghai Jiao Tong University School of Medicine
Yan-Tao Wei	Zhongshan Ophthalmic Center, Sun Yat-sen University
Yin Shen	Renmin Hospital of Wuhan University
Yong Tao	Beijing Chaoyang Hospital, Capital Medical University
Wei-Hua Yang	Shenzhen Eye Hospital, Shenzhen Eye Disease Prevention and Treatment Institute

Guang-Hui Liu	Affiliated People's Hospital (Fujian Provincial People's Hospital), Fujian University of Traditional Chinese Medicine
Ren-Zhe Cui	The Affiliated Hospital of Yanbian University
Su Zhao	The Affiliated Hospital of Guizhou Medical University
Hui Zhang	The First Affiliated Hospital of Kunming Medical University
Dan Ji	Xiangya Hospital of Central South University
Zhao-An Su	Zhejiang University, Eye Center of Second Affiliated Hospital, School of Medicine
Jian-Qi Cai	China National Institute of Standardization
Liang Hu	Eye Hospital of Wenzhou Medical University
Yao Yu	The First Affiliated Hospital of Nanchang University
Ting-Ting Shao	Eye and ENT Hospital of Fudan University
Wen-Jin Zou	The First Affiliated Hospital of Guangxi Medical University
Yi Liu	Nanjing Hospital of Chinese Medicine Affiliated to Nanjing University of Chinese Medicine
Juan Peng	The Second Affiliated Hospital of Guangzhou Medical University
Cheng Li	Eye Institute of Xiamen University
Shi-Ying Li	The First Affiliated Hospital of Xiamen University
Zhong-Wen Li	Ningbo Eye Hospital
Lei Tian	Beijing Tongren Hospital, Capital Medical University
Rui-Bo Yang	Tianjin Medical University Eye Hospital
Dan Wen	Xiangya Hospital of Central South University
Zhi-Hong Deng	The Third Xiangya Hospital of Central South University
Xuan Liao	Affiliated Hospital of North Sichuan Medical College
Gang-Jin Kang	The Affiliated Hospital of Southwest Medical University
Xiu-Sheng Song	The Central Hospital of Enshi Tujia and Miao Autonomous Prefecture
Wen-Qing Shi	Jinshan Hospital of Fudan University
Qian-Min Ge	The First Affiliated Hospital of Nanchang University
Mu Qin	The Affiliated Hospital of Xiangnan University
Xia Hua	Aier Eye Hospital (Tianjin)
Yi-Ping Jiang	The First Affiliated Hospital of Gannan Medical University
Hong-Ling Liu	The First Affiliated Hospital of Harbin Medical University
Zheng-Ri Li	Affiliated Hospital of Yanbian University
Cheng-Wei Lu	First Bethune Hospital of Jilin University

Hua-Tao Xie	Union Hospital, Tongji Medical College, Huazhong University of Science and Technology
He Dong	The Third People's Hospital of Dalian&Dalian Municipal Eye Hospital
Yang Liu	Zhongnan Hospital of Wuhan University
Yong Wang	Aier Eye Hospital (Wuhan)
Feng Wang	Meizhou People's Hospital
Mu-Di Yao	Shanghai General Hospital of Shanghai Jiao Tong University School of Medicine
Jia-Li Wu	Shanghai General Hospital of Shanghai Jiao Tong University School of Medicine
Xi-Jian Dai	The Second Affiliated Hospital of Nanchang University
Jing Wang	Shanghai General Hospital of Shanghai Jiao Tong University School of Medicine
Yong-Zhi Huang	West China Hospital of Sichuan University
Li-Jun Ji	Shanghai Dahua Hospital
Chuan-Bao Li	The First Affiliated Hospital of Jining Medical College
Yang Jie	Beijing Tongren Hospital, Capital Medical University
Chun-Ling Liu	West China Hospital, Sichuan University
Xue-Zhi Zhou	Xiangya Hospital, Central South University
Qi-Bin Xu	The First Affiliated Hospital of Jiujiang University
Bin Li	Xinhua Hospital Affiliated to Shanghai Jiao Tong University School of Medicine
Jia He	Jining Medical University
Li-Juan Luo	Xiaoshan Hospital, Affiliated with Hangzhou Normal University

### **Writing experts**

Meng-Tian Bai	Suining Central Hospital
Dan-Min Cao	The First Affiliated Hospital of Guangzhou Medical University
Yong Chai	Jiangxi Children's Hospital
Cheng Chen	The First Affiliated Hospital of Nanchang University
Jing-Yao Chen	The First People's Hospital of Kunming
Jun Chen	Jiangxi University of Chinese Medicine
Xu Chen	Maastricht University, the Netherlands
Yan Chen	Aier Eye Hospital (Shanghai)
Zhe Cheng	Aier Eye Hospital (Changsha)
De-Yong Deng	Yueyang Hospital of Integrated Traditional Chinese and Western Medicine, Shanghai University of Traditional Chinese Medicine

Yu-Qing Deng	Zhongshan Ophthalmic Center, Sun Yat-sen University
Jing Dong	First Hospital of Shanxi Medical University
Zhi-Xin Geng	Beijing XianWei Medical Technology Co., Ltd.
Yi Han	Eye Institute of Xiamen University
Xin He	The First Affiliated Hospital of Xiamen University
Li-Dan Hu	Children's Hospital of Zhejiang University School of Medicine
Jin-Yu Hu	The First Affiliated Hospital of Nanchang University
Xiao-Qin Hu	Affiliated Eye Hospital of Nanchang University
Cai-Hong Huang	Eye Institute of Xiamen University
Ming-Hai Huang	Aier Eye Hospital (Nanning)
Xiao-Ming Huang	Sichuan Eye Hospital
Xu Huang	Hangzhou Huaxia Eye Hospital
Hong-Hua Kang	Eye Institute of Xiamen University
Xiang-Yi Liu	The First Affiliated Hospital of Nanchang University
Hsuanyi Lee	Columbia University
En-Hui Li	Taizhou Hospital of Zhejiang Province
Hai-Bo Li	Xiamen Eye Center of Xiamen University
Heng-Hui Li	The First Affiliated Hospital of Nanchang University
Jie Li	Eye Hospital of Wenzhou Medical University
Kai-Jun Li	Shenzhen Eye Hospital, Affiliated with Southern Medical University
Nai-Yang Li	Zhongshan City People's Hospital
Qing-Jian Li	Huashan Hospital, Fudan University
Zhi-Yuan Li	The First People's Hospital of Chenzhou
Rong-Bin Liang	Jinshan Hospital of Fudan University
Zhi-Rong Lin	Xiamen Eye Center, Xiamen University
Qian Ling	The First Affiliated Hospital of Nanchang University
Jun Liu	The 924th Hospital of the Joint Logistics Support Force of the Chinese People's Liberation Army
Qiu-Ping Liu	The First Affiliated Hospital of University of South China
Ting-Ting Liu	Eye Hospital of Shandong First Medical University
Zu-Guo Liu	Eye Institute of Xiamen University
Wei Ma	Zhongshan ophthalmic Center, Sun Yat-sen University
Ren-Jie Miao	The Second Affiliated Hospital Zhejiang University School of Medicine

Shang-Kun Ou	The Affiliated Hospital of Guizhou Medical University
Wei-Jie Ouyang	The Affiliated Hospital of Guizhou Medical University
Kun-Liang Qiu	Joint Shantou International Eye Center of Shantou University and the Chinese University of Hong Kong
Wei-Qiang Qiu	Peking University Third Hospital
Sheng-Wei Ren	Henan Eye Hospital
Yi-Lei Shao	Eye Hospital of Wenzhou Medical University
Ting Su	Renmin Hospital of Wuhan University
Lei Tang	The Third People's Hospital of Yibin
Li-Ying Tang	Zhongshan Hospital, Xiamen University
Li-Yang Tong	Wenzhou Medical University Ningbo Eye Hospital
He Wang	The Affiliated Hospital of Xuzhou Medical University
Shen Wang	The First Affiliated Hospital of Xinxiang Medical University
Shao-Pan Wang	Institute of Artificial Intelligence, Xiamen University
Shu-Rong Wang	The Third Bethuen Hospital of Jilin University
Xiao-Yu Wang	The First Affiliated Hospital of Nanchang University
Xue-Lin Wang	The First Affiliated Hospital of Jiangxi Medical College
Hong Wei	The First Affiliated Hospital of Nanchang University
Xin Wen	Sun Yat-sen Memorial Hospital, Sun Yat-sen University
Wei Wu	Chinese PLA General Hospital
Kai Wu	The First Affiliated Hospital of University of South China
Yang Wu	Zhongshan Hospital, Fudan University (Xiamen Branch)
Wei Xia	The First Affiliated Hospital of Soochow University
Ang Xiao	The First Affiliated Hospital of Nanchang University
Yi-Chen Xiao	Eye and ENT Hospital of Fudan University
Ren-Yi Xie	Xiamen Eye Center of Xiamen University
San-Hua Xu	The First Affiliated Hospital of Nanchang University
Yang Yang	Yueyang Central Hospital
Yong Yao	C-MER (Guangzhou) Dennis Lam Eye Hospital
Hai-Jun Yang	Nanchang Bright Eye Hospital
Qi-Chen Yang	West China Hospital of Sichuan University
Shu Yang	The First People's Hospital of Kunming
Yi-Ran Yang	Henan Eye Hospital

Yu-Li Yang	The Southwest Hospital of Army Medical University
Yi-Feng Yu	The Second Affiliated Hospital of Nanchang University
Qing Yuan	Jiujiang First People's Hospital
Yan-Mei Zeng	The First Affiliated Hospital of Nanchang University
Qing Zhang	The Second Hospital of Anhui Medical University
Yu-Qing Zhang	The Second Affiliated Hospital of Chongqing Medical University
Yu-Jie Zhang	Xiamen Eye Center of Xiamen University
Zhen Zhang	The First Affiliated Hospital of Xiamen University
Zhen-Hao Zhang	Shanghai University of Medicine and Health Sciences Affiliated Zhoupu Hospital
Jing Zhong	Zhongshan Ophthalmic Center, Sun Yat-sen University
Pei-Wen Zhu	Eye and ENT Hospital of Fudan University
Zhuo-Ting Zhu	Eye Center of the University of Melbourne
Jie Zou	The First Affiliated Hospital of Nanchang University

## REFERENCES

- Huang D, Swanson EA, Lin CP, Schuman JS, Stinson WG, Chang W, Hee MR, Flotte T, Gregory K, Puliafito CA, et al.: Optical coherence tomography. *Science* 1991, 254:1178-1181.
- Schuman JS, Hee MR, Arya AV, Pedut-Kloizman T, Puliafito CA, Fujimoto JG, Swanson EA: Optical coherence tomography: a new tool for glaucoma diagnosis. *Curr Opin Ophthalmol* 1995, 6:89-95.
- Dauerman HL: Optical Coherence Tomography - Light and Truth. *N Engl J Med* 2023, 389:1523-1525.
- Gao SS, Jia Y, Zhang M, Su JP, Liu G, Hwang TS, Bailey ST, Huang D: Optical Coherence Tomography Angiography. *Invest Ophthalmol Vis Sci* 2016, 57:Oct27-36.
- Zhang A, Zhang Q, Chen CL, Wang RK: Methods and algorithms for optical coherence tomography-based angiography: a review and comparison. *J Biomed Opt* 2015, 20:100901.
- Ang M, Tan ACS, Cheung CMG, Keane PA, Dolz-Marco R, Sng CCA, Schmetterer L: Optical coherence tomography angiography: a review of current and future clinical applications. *Graefes Arch Clin Exp Ophthalmol* 2018, 256:237-245.
- Bergeron S, Miyamoto D, Sanft DM, Burnier JV, Mastromonaco C, Romano AA, Arthurs B, Burnier MN, Jr.: Novel application of anterior segment optical coherence tomography for periocular imaging. *Can J Ophthalmol* 2019, 54:431-437.
- Kishi S: Impact of swept source optical coherence tomography on ophthalmology. *Taiwan J Ophthalmol* 2016, 6:58-68.
- Podoleanu AG: Optical coherence tomography. *J Microsc* 2012, 247:209-219.
- Ehlers N, Hjortdal J: Corneal thickness: measurement and implications. *Exp Eye Res* 2004, 78:543-548.
- Tao A, Shao Y, Zhong J, Jiang H, Shen M, Wang J: Versatile optical coherence tomography for imaging the human eye. *Biomed Opt Express* 2013, 4:1031-1044.
- Meek KM, Knupp C: Corneal structure and transparency. *Prog Retin Eye Res* 2015, 49:1-16.
- Müller LJ, Marfurt CF, Kruse F, Tervo TM: Corneal

nerves: structure, contents and function. *Exp Eye Res* 2003, 76:521-542.

Kojima T, Tamaoki A, Yoshida N, Kaga T, Suto C, Ichikawa K: Evaluation of axial length measurement of the eye using partial coherence interferometry and ultrasound in cases of macular disease. *Ophthalmology* 2010, 117:1750-1754.

Wolffsohn JS, Kollbaum PS, Berntsen DA, Atchison DA, Benavente A, Bradley A, Buckhurst H, Collins M, Fujikado T, Hiraoka T, et al: IMI - Clinical Myopia Control Trials and Instrumentation Report. *Invest Ophthalmol Vis Sci* 2019, 60:M132-m160.

Brás JEG, Sickenberger W, Hirnschall N, Findl O: Cataract quantification using swept-source optical coherence tomography. *J Cataract Refract Surg* 2018, 44:1478-1481.

Huang J, Chen H, Li Y, Chen Z, Gao R, Yu J, Zhao Y, Lu W, McAlinden C, Wang Q: Comprehensive Comparison of Axial Length Measurement With Three Swept-Source OCT-Based Biometers and Partial Coherence Interferometry. *J Refract Surg* 2019, 35:115-120.

Grünert U, Martin PR: Cell types and cell circuits in human and non-human primate retina. *Prog Retin Eye Res* 2020:100844.

Chu Z, Lin J, Gao C, Xin C, Zhang Q, Chen CL, Roisman L, Gregori G, Rosenfeld PJ, Wang RK: Quantitative assessment of the retinal microvasculature using optical coherence tomography angiography. *J Biomed Opt* 2016, 21:66008.

Masland RH: The fundamental plan of the retina. *Nat Neurosci* 2001, 4:877-886.

Hoon M, Okawa H, Della Santina L, Wong RO: Functional architecture of the retina: development and disease. *Prog Retin Eye Res* 2014, 42:44-84.

Liang X, Graf BW, Boppart SA: Imaging engineered tissues using structural and functional optical coherence tomography. *J Biophotonics* 2009, 2:643-655.

Chen CL, Wang RK: Optical coherence tomography based angiography [Invited]. *Biomed Opt Express* 2017, 8:1056-1082.

Le PH, Kaur K, Patel BC: Optical Coherence Tomography Angiography. In *StatPearls*. Treasure Island (FL) ineligible companies. Disclosure: Kirandeep Kaur declares no relevant financial relationships with ineligible companies. Disclosure: Bhupendra Patel declares no relevant financial relationships with ineligible companies.; 2025

Koustenis A, Jr., Harris A, Gross J, Januleviciene I, Shah A, Siesky B: Optical coherence tomography angiography: an overview of the technology and an assessment of applications for clinical research. *Br J Ophthalmol* 2017, 101:16-20.

Jia Y, Tan O, Tokayer J, Potsaid B, Wang Y, Liu JJ, Kraus MF, Subhash H, Fujimoto JG, Hornegger J, Huang D: Split-spectrum amplitude-decorrelation angiography with optical coherence tomography. *Opt Express* 2012, 20:4710-4725.

Freddo TF: Ultrastructure of the iris. *Microsc Res Tech* 1996, 33:369-389.

Iovino C, Peiretti E, Braghiroli M, Tatti F, Aloney A, Lanza M, Chhablani J: Imaging of iris vasculature: current limitations and future perspective. *Eye (Lond)* 2022, 36:930-940.

Bharadwaj AS, Appukuttan B, Wilmarth PA, Pan Y, Stempel AJ, Chipps TJ, Benedetti EE, Zamora DO, Choi D, David LL, Smith JR: Role of the retinal vascular endothelial cell in ocular disease. *Prog Retin Eye Res* 2013, 32:102-180.

Bek T: Regional morphology and pathophysiology of retinal vascular disease. *Prog Retin Eye Res* 2013, 36:247-259.

Nickla DL, Wallman J: The multifunctional choroid. *Prog Retin Eye Res* 2010, 29:144-168.

Wu H, Zhang G, Shen M, Xu R, Wang P, Guan Z, Xie Z, Jin Z, Chen S, Mao X, et al: Assessment of Choroidal Vasculature and Choriocapillaris Blood Perfusion in Anisomyopic Adults by SS-OCT/OCTA. *Invest Ophthalmol Vis Sci* 2021, 62:8.

Bermudez MA, Vicente AF, Romero MC, Arcos MD, Abalo JM, Gonzalez F: Time course of cold cataract development in anesthetized mice. *Curr Eye Res* 2011,

36:278-284.

Liu X, Wang CH, Dai C, Camesa A, Zhang HF, Jiao S:  
Effect of contact lens on optical coherence tomography  
imaging of rodent retina. *Curr Eye Res* 2013, 38:1235-1240.

Kirihara Y, Takechi M, Kurosaki K, Kobayashi Y, Saito Y,  
Takeuchi T: Anesthetic effects of a three-drugs mixture--  
comparison of administrative routes and antagonistic  
effects of atipamezole in mice. *Exp Anim* 2015, 64:39-47.

Kashani AH, Chen CL, Gahm JK, Zheng F, Richter GM,  
Rosenfeld PJ, Shi Y, Wang RK: Optical coherence  
tomography angiography: A comprehensive review of  
current methods and clinical applications. *Prog Retin Eye  
Res* 2017, 60:66-100.

Lee J, Rosen R: Optical Coherence Tomography  
Angiography in Diabetes. *Curr Diab Rep* 2016, 16:123.

Liu L, Xia F, Hua R: Retinal nonperfusion in optical  
coherence tomography angiography. *Photodiagnosis  
Photodyn Ther* 2021, 33:102129.